

See discussions, stats, and author profiles for this publication at: <https://www.researchgate.net/publication/23251821>

Metal Al Produced by H₂ Plasma Reduction of AlCl₃ : A Thermodynamic and Kinetic Study on the Plasma Chemistry

ARTICLE in THE JOURNAL OF PHYSICAL CHEMISTRY B · OCTOBER 2008

Impact Factor: 3.3 · DOI: 10.1021/jp8035204 · Source: PubMed

CITATIONS

7

READS

17

6 AUTHORS, INCLUDING:



Jie Zheng

Peking University

81 PUBLICATIONS 1,287 CITATIONS

SEE PROFILE

Rong Yang

General Research Institute for Nonferrous ...

32 PUBLICATIONS 696 CITATIONS

SEE PROFILE

Metal Al Produced by H₂ Plasma Reduction of AlCl₃: A Thermodynamic and Kinetic Study on the Plasma Chemistry

Jie Zheng,[†] Bo Sun,[†] Rong Yang,[†] Xubo Song,[†] Xingguo Li,^{*,†,‡} and Yikang Pu[§]

Beijing National Laboratory for Molecular Sciences (BNLMS) (The State Key Laboratory of Rare Earth Materials Chemistry and Applications), College of Chemistry and Molecular Engineering, Peking University, Beijing, P.R. China, 100871, College of Engineering, Peking University, Beijing, P.R. China, 100871, Department of Engineering Physics, Tsinghua University, Beijing, P.R. China, 100084

Received: April 23, 2008; Revised Manuscript Received: July 1, 2008

In this paper we reported that low temperature plasma may reverse the direction of a chemical reaction. The thermodynamically forbidden reaction between H₂ and AlCl₃ was able to take place with the assistance of low temperature plasma, yielding metal Al. The plasma chemistry of the reaction was investigated by optical emission spectroscopy, which suggested that the dissociation of H₂ and AlCl₃ molecules by plasma led the reaction to a thermodynamically favorable one by creating reaction channels with low Gibbs free energy change. The addition of Ar promoted the reaction kinetics dramatically, which was attributed to the enhanced dissociation of AlCl₃ molecules by excited Ar species.

Introduction

Application of plasma in chemical reactions has intrigued long lasting research interest because of its wide application, especially its particular importance in semiconductor industries.^{1–3} Often referred as “plasma enhanced” chemical reactions, plasma is capable of accelerating chemical reactions owing to its high chemical reactivity. Plasma enhanced chemical vapor deposition (PECVD) technique has been applied to produce a large variety of materials with high deposition rate, including silicon (both amorphous⁴ and crystalline⁵), carbon (diamond,⁶ diamond-like carbon,⁷ and carbon nanotubes⁸), oxides,⁹ nitrides¹⁰ and carbides.¹¹ In contrast to the pronounced kinetic effects of plasma exhibited in a large number of chemical reactions, the insights into the thermodynamic aspect of plasma chemistries are still rare. Whether plasma is able to make a thermodynamically unfavorable chemical reaction happen, as it does for kinetically unfavorable ones is still not well studied. Especially, there is lack of examples showing the substantial thermodynamic effects of plasma up to now. Plasma does show some thermodynamic effects on some reactions. For example, in preparation of carbon based materials, plasma causes hydrocarbon molecules to crack at much lower temperature than thermodynamics predicts. However, in these cases, plasma serves mainly as an alternative energy source to the conventional heating^{12,13} and is not a determining factor for the reaction thermodynamics.

In this paper we demonstrate the significance of plasma on reaction thermodynamics using the reaction between AlCl₃ and H₂, which is thermodynamically forbidden even at temperature exceeding 1000 °C.^{14,15} Using radio frequency plasma, metal Al could be produced at high rate around 100 °C. Addition of Ar into the reaction system significantly enhanced the reaction kinetics. The plasma chemistry of the reaction was studied by optical emission spectroscopy (OES), based on which the effects

of plasma on the thermodynamics and kinetics were discussed. In addition to a demonstration of the substantial thermodynamic effect of plasma, the plasma reaction presented in this paper also has technological importance. Reduction of metal chlorides by hydrogen has been used to prepare a large variety of metals and alloys.^{16–18} However, the preparation of Al and its alloy is difficult owing to the thermodynamic limitations.^{14,19} The H₂ plasma enhanced reduction reaction presented in this paper may provide a new method to prepare elements and alloys of reactive metals.

Experimental Section

The experimental setup is schematically illustrated in Figure 1, which consisted of a horizontal quartz tube (2.8 cm in diameter and 100 cm in length) and an inductively coupled coil (10 cm in length) surrounding the tube. The coil was driven by a 13.56 MHz, 500 W radio frequency power source. 0.6 g AlCl₃ anhydrous (98%, Beijing Yili Chemical Factory) was loaded in a small one-end sealed glass tube (5 cm in length and 1 cm in diameter). The glass tube was inserted horizontally into the quartz tube 4 cm upstream the coil, with its sealed end pointing downstream. A mercury thermometer was inserted into the AlCl₃ powder to monitor the exact temperature. There are six pinholes at the sealed end to regulate the evaporation rate of AlCl₃. One piece of 2 × 2 cm² glass were placed at 3 cm downstream of the AlCl₃ powder as the substrate. The whole quartz tube was evacuated to 0.6 Pa by a rotary pump and was flushed with Ar (99.99%) several times to remove oxygen and moisture. The AlCl₃ powder was heated by a heating tape under a mixture gas flow of Ar and H₂ (99.99%). The AlCl₃ evaporation temperature was controlled at 90 °C to ensure stable AlCl₃ evaporation. The H₂ flow was 30 sccm and the chamber pressure was regulated so that the H₂ partial pressure was kept at 20 Pa. After the temperature reached 90 °C as read from the mercury thermometer, plasma was ignited, showing a bright pale blue glow (Figure 2b). The rf power was kept at 100 W. The temperature of the substrate was about 100 °C due to combined effects of the heating tape and the rf coil, as measured by a mercury thermometer without the AlCl₃ source. After 20 min,

* Corresponding author. E-mail: xgli@pku.edu.cn.

[†] Beijing National Laboratory for Molecular Sciences (BNLMS) (The State Key Laboratory of Rare Earth Materials Chemistry and Applications), College of Chemistry and Molecular Engineering, Peking University.

[‡] College of Engineering, Peking University.

[§] Department of Engineering Physics, Tsinghua University.

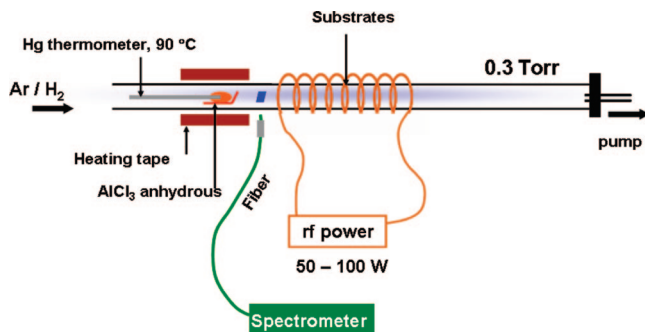


Figure 1. Schematic illustration of the ICP reaction setup.

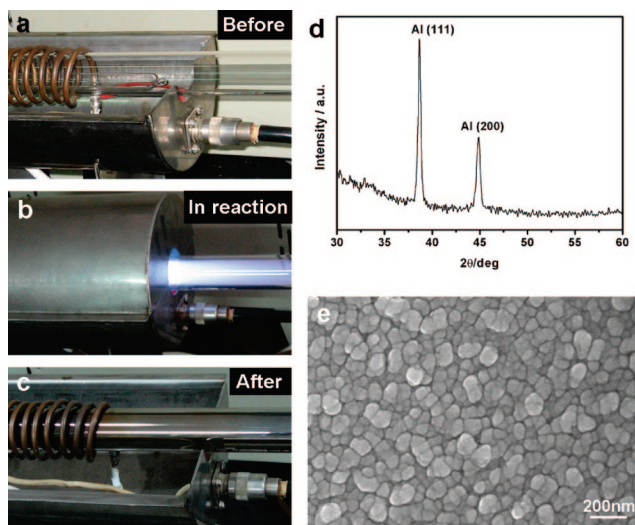


Figure 2. (a–c) Photographs of the reaction setup before, during and after reaction, showing a pale blue glow of AlCl₃ plasma and metallic coating after reaction. (d) XRD pattern of the deposition. (e) SEM image of the deposition.

the heating tape was removed from the AlCl₃ area. The plasma was switched off when the AlCl₃ temperature cooled down to 40 °C (in about 10 min). The heating procedure used in the experiment resulted in an average AlCl₃ evaporation rate of 0.1 mmol min⁻¹, as measured from the AlCl₃ mass loss after reactions. A shining metallic layer was coated on the inner wall of the quartz tube. The product collected on the substrate was examined by X-ray diffraction (XRD, Rigaku Dmax 200, Cu Ka) and scanning electron microscopy (SEM, Hitachi S4800, 10kV). The amount of deposited Al was calculated by dissolving the deposition in 1 M HCl and subsequent measurement of the Al concentration in the solution by inductively coupled plasma-atomic emission spectroscopy (ICP-AES, Leeman Profile).

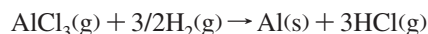
In situ plasma optical emission spectra were collected using a fiber spectrometer (Avantes 2048) at the substrate position. Spectra could only be collected in the first 30 s because the deposition of Al on the tube wall no longer allowed the access of the plasma emission from the side. The OES spectra of Ar–H₂ mixture and Ar–AlCl₃ with the same configuration as the deposition experiments were also collected for thermodynamic and kinetic study.

Results and Discussion

The formation of metal Al was evident, as confirmed by both the metallic shining of the product (Figure 2c) and the XRD pattern (Figure 2d). According to the XRD pattern, Al was also the only product. The deposited Al was in the form of thin films composed of fine particles around 100 nm, as seen from the

SEM image (Figure 2e). The conversion of AlCl₃ should be close to 100% since no solid AlCl₃ condensed in the low temperature area was observed, though the exact quantity was difficult to estimate. Without plasma, nothing happened except that the unreacted AlCl₃ condensed at the low temperature part of the quartz tube.

Apparently, with the assistance of plasma, the follow reaction took place at about 100 °C



This reaction is thermodynamically forbidden because the Gibbs free energy change is a very large positive value (284.7 kJ·mol⁻¹). The formation free energy $\Delta_f G^\circ$ at 298 K of AlCl₃ and HCl in the gas state is -570.6 and -95.30 kJ·mol⁻¹, respectively^{15,20}. Even raising the reaction temperature up to 1000 °C does not change the thermodynamic much.¹⁴ The effect of plasma on the thermodynamics is significant.

Formation of metal Al in this reaction requires that the Al concentration in the gas phase exceeds certain critical value (at least the saturated Al vapor pressure at the reaction temperature). Once the solid phase Al was formed and removed from the gas phase, it can not be converted to AlCl₃ and back to the gas phase again, because the product HCl was continuously pumped away.

Consider the reaction: $\text{AlCl}_3 + 3/2\text{H}_2 \rightarrow \text{Al} + 3\text{HCl}$ in which all the matters involved are in the gas phase. The Al concentration is determined by the equilibrium equation

$$\frac{n_{\text{Al}} n_{\text{HCl}}^3}{n_{\text{H}_2}^{1.5} n_{\text{AlCl}_3}} = K = \exp\left(-\frac{\Delta G}{k_B T}\right) \quad (1)$$

where n indicates the equilibrium gas phase concentration of the species denoted by the corresponding subscript, K is the equilibrium constant, ΔG is the Gibbs free energy change, k_B is the Boltzmann constant, and T is the reaction temperature.

Note $n_{\text{HCl}} = 3n_{\text{Al}}$, which gives

$$n_{\text{Al}} = \left(\frac{n_{\text{H}_2}^{1.5} n_{\text{AlCl}_3}}{27} \right)^{1/4} \exp\left(-\frac{\Delta G}{4k_B T}\right) \quad (2)$$

Since the concentrations of H₂ and AlCl₃ are fixed by H₂ gas flow and AlCl₃ evaporation temperature, the gas phase Al concentration is solely determined by ΔG . The large positive ΔG without plasma leads to very small gas phase Al concentration (10⁻² cm⁻³, estimated by using $n_{\text{H}_2} = 10^{15}$ cm⁻³ and $n_{\text{AlCl}_3} = 10^{13}$ cm⁻³, according to their flow rate and the partial pressure of H₂), below the threshold of solid Al formation. Thus, no solid phase Al was formed.

Almost all the species are in the electronic ground-state at 100 °C in the nonplasma reaction. When plasma is introduced, excited states created by plasma have to be taken into account. Optical emission spectroscopy (OES) is a useful technique to qualitatively identify the excited species. As shown in Figure 3, three Balmer lines of H atoms (H_α , 656.6 nm; H_β , 486.0 nm; H_γ , 343 nm) could be clearly identified in the spectrum. Spikes originated from the emission of AlCl radicals^{21–23} (261 nm) and Al atoms²⁴ (308 and 396 nm) were observed in the short wavelength region. No discernible emission from Cl atoms was observed.²⁴ Therefore, the excited species created by plasma are mainly AlCl radicals, Al atoms and H atoms through the dissociation of AlCl₃ and H₂. This dissociation is rather inefficient by heating.²³ Despite of the intense emission, the dissociation degree was quite low, typically 10⁻⁴ to 10⁻² for H₂.^{25,26}

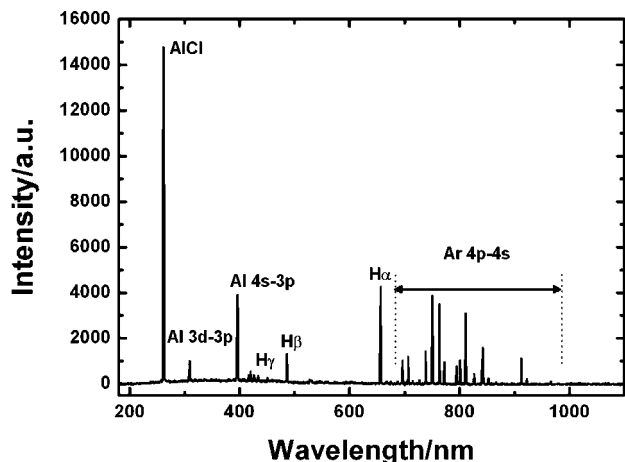


Figure 3. A typical OES spectrum of the $\text{AlCl}_3\text{-H}_2\text{-Ar}$ system.

Including the excited species, additional reaction channels with lower ΔG were available. The most important one was $\text{AlCl} + \text{H} \rightarrow \text{Al} + \text{HCl}$, since AlCl and H were the dominant excited species according to the OES results. The ΔG of this reaction was roughly the difference of the bond energy of Al-Cl ($494 \text{ kJ}\cdot\text{mol}^{-1}$) and H-Cl ($432 \text{ kJ}\cdot\text{mol}^{-1}$),²⁰ which is a much smaller positive value ($62 \text{ kJ}\cdot\text{mol}^{-1}$) compared to the nonplasma process. The equilibrium Al atom concentration is given by a similar exponential expression

$$n_{\text{Al}} = \left(\frac{n_{\text{H}} n_{\text{AlCl}}}{4} \right)^{1/2} \exp\left(-\frac{\Delta G}{2k_{\text{B}}T}\right) \quad (3)$$

The much smaller ΔG value gives higher equilibrium Al atom concentration. Assuming 0.1% dissociation ratio of both H_2 and AlCl_3 which is typical for the plasma operating in the experimental conditions, the equilibrium concentration of Al atoms is estimated to be 10^6 cm^{-3} , 8 orders of magnitude higher than that of the nonplasma case. In a macroscopic energy point of view, the plasma helped to break two Al-Cl bonds and one H-H bond for each reaction, resulting in a large energy gain toward the solid Al formation.

Another reaction $\text{AlCl} \rightarrow \text{Al} + \text{Cl}$ also yielded Al atoms in the gas phase and was readily observed by OES. However, it could not be the main reason for the substantial equilibrium Al increase because the ΔG of this reaction is still large, in agreement with the lack of metal Al formation in $\text{AlCl}_3\text{-Ar}$ plasma.

In summary, due to the excited states created by plasma, the reaction could proceed through some channels with lower ΔG . The overall effect showed a decrease of free energy change, which gave higher equilibrium Al atom concentration in the gas phase.

The Al deposition rate in pure H_2 was estimated to be $6.5 \text{ mg}\cdot\text{cm}^{-2}\cdot\text{s}^{-1}$, according to the amount of Al deposited on the glass substrate measured by ICP-AES. The Al deposition rate could be significantly enhanced when Ar is introduced into the system. To quantitatively estimate the effect of Ar on the kinetics, the H_2 flow was kept at 30 sccm and the Ar flow increase from 0 to 60 sccm. The chamber pressure was regulated to maintain the H_2 partial pressure at 20 Pa so that the amount of reactive gas was the same for each run. The deposition rate at different Ar flows is shown in Figure 4a, showing a monotonic increase with increasing Ar flow. Although Ar is an inert species in most chemical reactions, it clearly served as a kinetic promoter here. The error in each data point was about 15%, as estimated from 3 repeated runs at each Ar flow.

The kinetic effects of Ar are also studied by OES. Because the deposition of Al on the quartz tube made the systematic

collection of the $\text{AlCl}_3\text{-H}_2\text{-Ar}$ mixture spectra impossible, we studied the effects of Ar addition on H_2 and AlCl_3 separately by looking into Ar-H_2 and Ar-AlCl_3 spectra taken at different Ar flows (Figure 4b,c). The intensity of the H atomic lines decreased when more Ar was introduced (Figure 4b), indicating the decrease of H atom density caused by Ar addition. This can be easily understood as the power dilution effect, since the power imposed on H_2 molecules became lower for lower H_2 fraction when the input power was fixed. The electron temperature could be estimated based on the relative intensity of the atomic hydrogen lines. Higher $\text{H}\beta/\text{H}\alpha$ ratio means higher population at higher excited levels, which also indicated higher electron energy if assuming that the excitation of H atoms is mainly caused by electron impact. More accurately, the emission intensity could be written as²⁷

$$I_{j \rightarrow k} = \frac{A_{jk} g_j}{\lambda_{jk}} \exp\left(-\frac{E_j - E_k}{k_{\text{B}} T_e}\right)$$

where $I_{j \rightarrow k}$ is the line intensity corresponding to the transition from higher energy level j to lower one k , A_{jk} is the corresponding transition probability, λ_{jk} is the wavelength of the transition, $E_j - E_k$ is the energy difference between level j and level k , g_j is the statistic weight (or degeneracy) of the higher energy level, k_{B} is the Boltzmann constant, and T_e is the electron temperature.

Using well established transition probability values of H atoms²⁸ and plotting $I_{j \rightarrow k} \lambda_{jk} / A_{jk} g_j$ against $E_j - E_k$, T_e can be obtained.²⁹ The statistic weight of the higher energy levels of $\text{H}\alpha$, $\text{H}\beta$, and $\text{H}\gamma$ are 18, 32, and 50, corresponding to the principle quantum number 3, 4, and 5, respectively. The results were plotted in Figure 4b, showing a slight decrease with increasing Ar. This could be attributed to the suppression of lower energy electron loss rather than consumption of high energy electrons.³⁰ The electron density in Ar-H_2 plasma was known to increase with Ar fraction, because the most important electron loss channel $\text{ArH}^+ + \text{e} \rightarrow \text{Ar} + \text{H}$ is enhanced at higher H_2 fraction, resulting in the loss of some low energy electrons.²⁵ In addition, the presence of Ar could also generate low energy electrons through the ionization of H atoms by metastable Ar species (Ar^*): $\text{Ar}^* + \text{H} \rightarrow \text{Ar} + \text{H}^+ + \text{e}$. The decrease of H atom density and electron temperature with Ar addition is in agreement with the results obtained in capacitively coupled plasma³⁰ and direction current glow discharge.³¹ Obviously, Ar addition was not expected to enhance the reaction kinetic from the H_2 side, since neither the density of reactive H atoms was raised nor the electrons became more powerful.

As a direct deduction, the overall kinetic enhancement must be attributed to the positive effects on the AlCl_3 side caused by Ar Addition. The change of the AlCl_3 OES spectra due to Ar addition is shown in Figure 4c. Both the AlCl radical emission at 261 nm and the Al atom emission at 396 nm became more intense with raising Ar flow, while their ratio remained the same. The influence of Ar flow on the AlCl_3 evaporation was negligible in our experiment. The effect of Ar was mainly owing to the change of the plasma processes. The OES results suggested that the dissociation of AlCl_3 were enhanced at higher Ar flow.

Ar addition resulted in higher density of electrons, as discussed above, as well as Ar^+ and Ar^* , all of which were favorable for the dissociation of AlCl_3 molecules, through either direct electron impact or energy transfer from Ar ions and metastables. The dissociation enhanced by direct electron impact was not expected to be significant, since the extra electrons brought by Ar addition were low energy ones.³⁰ The energy transfer from the excited Ar species (Ar^* and Ar^+) were responsible for the enhancement of AlCl_3 dissociation. As shown

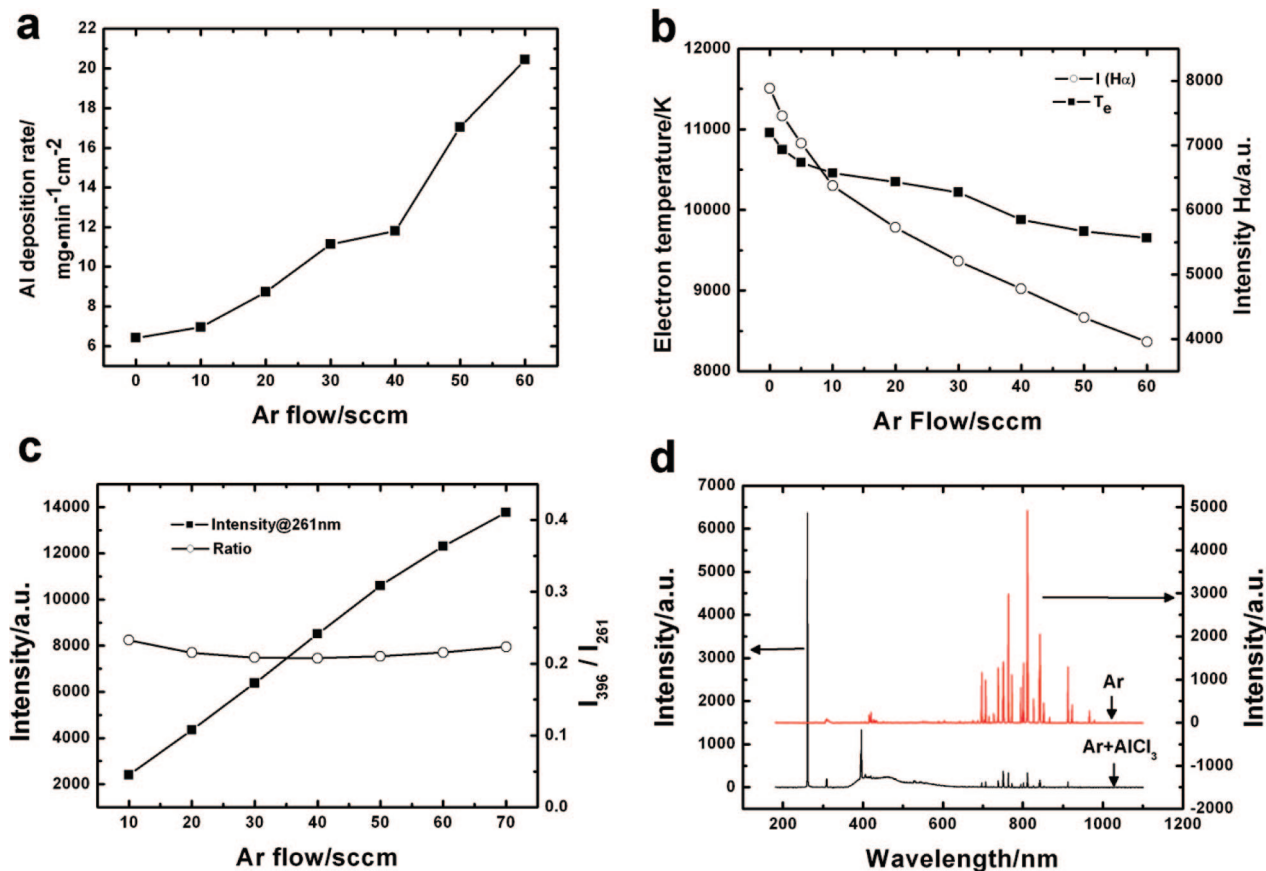
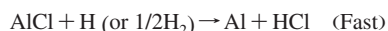
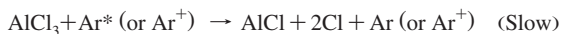


Figure 4. (a) Al deposition rate at different Ar flows. (b) Variation of the H_α line intensity (open circles) and electron temperature (filled squares) with the Ar flow in Ar–H₂ plasma. (c) Variation of the AlCl line intensity (filled squares) and the Al/AlCl intensity ratio (open circles) with the Ar flow in Ar–AlCl₃ plasma. (d) Comparison of pure Ar and Ar–AlCl₃ OES spectra, showing a significant decrease of Ar line intensity after the introduction of AlCl₃ vapor.

in Figure 4d, significant intensity drop of Ar 4p lines³² (700 to 1000 nm) and the relative intensity change among different Ar lines were observed when AlCl₃ vapor was introduced, suggesting efficient energy transfer between Ar* and AlCl₃ molecules. However, the OES results are only able to give a qualitative explanation. To quantitatively estimate the contribution from each energetic species, their number density, energy distribution and reaction cross sections need to be known, which requires combining other diagnostics with OES.

The addition of Ar caused a decrease of H atoms density but an increase of AlCl and Al density, together with an increase of low energy electron density. The overall enhancement of Ar on the kinetics suggested that the positive effects on the AlCl₃ dissociation outweighed the negative effects on the H₂ dissociation. A possible reason is that the dissociation of AlCl₃ molecules was the rate-limit step of this reaction. In the gas phase at the experimental temperature, AlCl₃ exists as dimers, in which the Al atoms are 4-fold coordinated by Cl atoms without any vacancies for electron transfer to the Al atoms. Breaking Al–Cl bonds would remove the stereo hindrance of the electron transfer from the H atoms or H₂ molecules to the Al atoms. Thus, reduction of AlCl radicals was much faster compared to that of Al₂Cl₆ dimers. A possible reaction mechanism for this plasma reaction is written as follows.



The assignment of the dissociation of AlCl₃ molecules being the rate-limit step is in agreement with the same trend of AlCl₃

dissociation and reaction kinetics caused by Ar addition according to the OES results. Here H₂ served as the reducing agent which was indispensable for the reaction. The free electrons in the plasma were too low in number density (typically 10¹¹ cm⁻³ for plasma operating at the experimental conditions²⁶) to serve as the reducing agent, as confirmed by the fact that the discharge of AlCl₃ in pure Ar plasma did not lead to any detectable metal Al formation.

Conclusion

We demonstrated the significant change in reaction thermodynamics caused by plasma in the reduction of AlCl₃ by H₂ plasma. Due to the species in excited electronic states created by plasma, reaction channels with lower free energy change were available, through which the thermodynamically forbidden reaction in non plasma conditions was able to take place. Addition of Ar promoted the reaction kinetics substantially, which is attributed to the enhancement of AlCl₃ dissociation caused by the excited Ar species. The plasma enhanced reduction discussed in this paper provides an effective new method to prepare reactive metals and their alloys.

Acknowledgment. This study was supported by the National Natural Science Foundation of China (Nos. 20221101 and 20671004), MOST of China (Nos. 2006AA05Z130, 2007AA05Z118) and MOE of China (No. 707002). Dr Li Zhang is highly appreciated for her kind support in the ICP-AES measurement.

References and Notes

- (1) Schram, D. C.; Vandermullen, J. A. M.; Vandesanden, M. C. M. *Plasma Phys. Control. Fusion* **1994**, *36*, B65–B78.

- (2) Cote, D. R.; Nguyen, S. V.; Stamper, A. K.; Armbrust, D. S.; Tobben, D.; Conti, R. A.; Lee, G. Y. *IBM J. Res. Dev.* **1999**, *43*, 5–38.
- (3) Layadi, N.; Colonell, J. I.; Lee, J. T. C. *Bell Labs Tech. J.* **1999**, *4*, 155–171.
- (4) Kessels, W. M. M.; Severens, R. J.; Smets, A. H. M.; Korevaar, B. A.; Adriaenssens, G. J.; Schram, D. C.; van de Sanden, M. C. M. *J. Appl. Phys.* **2001**, *89*, 2404–2413.
- (5) Cabarrocas, P. R. I. *J. Non-Cryst. Solids* **2000**, *266*, 31–37.
- (6) Kobashi, K.; Nishimura, K.; Kawate, Y.; Horiuchi, T. *Phys. Rev. B* **1988**, *38*, 4067–4084.
- (7) Grill, A.; Meyerson, B. S.; Patel, V. V. *IBM J. Res. Dev.* **1990**, *34*, 849–857.
- (8) Chhowalla, M.; Teo, K. B. K.; Ducati, C.; Rupasinghe, N. L.; Amaratunga, G. A. J.; Ferrari, A. C.; Roy, D.; Robertson, J.; Milne, W. I. *J. Appl. Phys.* **2001**, *90*, 5308–5317.
- (9) Martinu, L.; Poltras, D. *J. Vac. Sci. Tech. A* **2000**, *18*, 2619–2645.
- (10) Kessels, W. M. M.; Hong, J.; van Assche, F. J. H.; Moschner, J. D.; Lauinger, T.; Soppe, W. J.; Weeber, A. W.; Schram, D. C.; van de Sanden, M. C. M. *J. Vac. Sci. Tech. A* **2002**, *20*, 1704–1715.
- (11) Rajagopalan, T.; Wang, X.; Lahlouh, B.; Ramkumar, C.; Dutta, P.; Gangopadhyay, S. *J. Appl. Phys.* **2003**, *94*, 5252–5260.
- (12) Dai, H. J. *Acc. Chem. Res.* **2002**, *35*, 1035–1044.
- (13) Wang, T.; Xin, H. W.; Zhang, Z. M.; Dai, Y. B.; Shen, H. S. *Dia. Relat. Mater.* **2004**, *13*, 6–13.
- (14) Sohn, H. Y.; PalDey, S. J. *Mater. Res.* **1998**, *13*, 3060–3069.
- (15) Konings, R. J. M.; Booi, A. S. *J. Chem. Thermodyn.* **1992**, *24*, 1181–1188.
- (16) Park, K. Y.; Jang, H. D.; Choi, C. S. *J. Aero. Sci.* **1991**, *22*, S113–S116.
- (17) Jang, H. D.; Hwang, D. W.; Kim, D. P.; Kim, H. C.; Lee, B. Y.; Jeong, I. B. *Mater. Res. Bull.* **2004**, *39*, 63–70.
- (18) Zhao, G. Y.; Revankar, V. V. S.; Hlavacek, V. J. *Less-Common Met.* **1990**, *163*, 269–280.
- (19) Hasegawa, F.; Katayama, K.; Kobayashi, R.; Yamaguchi, H.; Nannichi, Y. *Jap. J. Appl. Phys. Part 2* **1988**, *27*, L254–L257.
- (20) Speight, J. G. *Lange's Handbook of Chemistry*, 16th ed.; Mc Graw-Hill: London, 2005.
- (21) Bhaduri, B. N.; Fowler, A. *Proc. R. Soc. London A* **1934**, *145*, 321–336.
- (22) Jevons, W. *Proc. R. Soc. London A* **1924**, *106*, 174–194.
- (23) Foster, L. M.; Russell, A. S.; Cochran, C. N. *J. Am. Chem. Soc.* **1950**, *72*, 2580–2587.
- (24) Sansonetti, J. E.; Martin, W. C. *J. Phys. Chem. Ref. Data* **2005**, *34*, 1559–2259.
- (25) Bogaerts, A.; Gijbels, R. *J. Anal. Atom. Spectrosc.* **2000**, *15*, 441–449.
- (26) Bogaerts, A. *J. Anal. Atom. Spectrosc.* **2002**, *17*, 768–779.
- (27) Mermet, J. M. *Inductively Coupled Plasmas: Emission Spectroscopy* Wiley: New York, 1987; Vol. 2.
- (28) Fuhr, J. R.; Wiese, W. L. NIST Atomic Transition Probabilities. In *CRC Handbook of Chemistry and Physics*, 71st ed.; CRC Press: Boca Raton, FL, 2005; pp128–179.
- (29) Darwiche, S.; Nikravec, M.; Awamat, S.; Morvan, D.; Amouroux, J. *J. Phys. D* **2007**, *40*, 1030–1036.
- (30) Laidani, N.; Bartali, R.; Tosi, P.; Anderle, M. *J. Phys. D* **2004**, *37*, 2593–2606.
- (31) Bogaerts, A.; Gijbels, R. *Spectrochim. Acta B* **2002**, *57*, 1071–1099.
- (32) Bogaerts, A.; Gijbels, R.; Vlcek, J. *Spectrochim. Acta B* **1998**, *53*, 1517–1526.

JP8035204